### JOHNSON MATTHEY TECHNOLOGY REVIEW

technology.matthey.com

# Investigation of Microstructural Characteristics and Mechanical Properties in Platinum-Rhodium Alloy Strengthened by Zirconium and Yttrium

Enhancing the high-temperature service performance of Pt-10Rh alloys

Changyi Hu<sup>1,2</sup>, Xiangxing Xiao<sup>1,2</sup>, Qianqi Wei<sup>1,2</sup>, Junmei Guo<sup>1,2</sup>, Xian Wang<sup>1,2</sup>, Li Chen<sup>1,2</sup>, Hongzhong Cai<sup>1,2</sup>, Xuehang Wang<sup>1,2</sup>, Xiaohong Yuan<sup>1,2</sup>, Yan Wei<sup>1,2</sup>\*, Zhentao Yuan<sup>3</sup>

<sup>1</sup>State Key Laboratory of Platinum Metal Functional Materials, Kunming Institute of Precious Metals, Kunming 650106, China

<sup>2</sup>Yunnan Precious Metals Laboratory Co Ltd, Kunming 650106, China

<sup>3</sup>School of Materials Science and Engineering, Kunming University of Science and Technology, Kunming 650051, China

Email: \*weiyan@ipm.com.cn

#### **PEER REVIEWED**

Received 3rd April 2024; Revised 30th July 2024; Accepted 13th August 2024; Online 14th August 2024

In pursuit of enhancing the high-temperature service performance of Pt-10Rh alloys, this study focuses on the preparation of two Pt-10Rh-based alloys through the incorporation of reinforcing elements zirconium and zirconium-yttrium. The investigation into the microstructure, mechanical properties and strengthening mechanisms of the alloys involved the utilisation of analytical tools

such as an optical metallographic microscopy (OM), X-ray diffraction (XRD), selected area electron diffraction (SAED), energy-dispersive X-ray spectroscopy (EDS) and tensile testing, coupled with first-principle computational analysis methods. The research results indicate the presence of Pt<sub>5</sub>Y precipitate phase and zirconium yttrium oxides in Pt-10Rh-0.5Zr-0.2Y alloy, but not detected in Pt-10Rh-0.5Zr alloy. It was found that adding a small amount of zirconium and yttrium elements to Pt-10Rh alloy can significantly enhance the mechanical properties at room temperature and 1300°C, especially the composite addition of zirconium and yttrium elements, which can also improve the high-temperature plasticity of the alloy. The strengthening mechanisms of zirconium and yttrium elements on Pt-10Rh alloy are mainly solid solution strengthening and second phase strengthening. The relationship between the mechanical properties of platinum-rhodium based alloys and their valence electron structure was discussed. The zirconium and yttrium reinforced platinum-rhodium based alloy studied in this work can replace Pt-10Rh alloy in certain fields.

#### 1. Introduction

Platinum-based alloys are distinguished by their outstanding corrosion resistance, catalytic activity, biocompatibility, creep strength and ductility, making them extensively utilised in aerospace, energy

conversion, medical devices and various other fields (1-3). Currently, platinum-rhodium alloys emerge as the most stable high-temperature alloys, demonstrating the ability to withstand oxidising environments at 1400°C for prolonged durations (4). The inclusion of rhodium in the alloy improves mechanical properties through mechanisms such as solid solution strengthening, dislocation introduction, phase hardening and alteration of the solid solution material's nature. These improvements align effectively with the service requirements of high strength and high-temperature stability (5, 6). Research indicates a substantial increase in the high-temperature mechanical properties of platinum-rhodium alloys with the escalation of rhodium content (7). However, when the rhodium content exceeds the threshold of 30 wt%, the observed enhancement of mechanical properties weakens, and the machinability also deteriorates (8). Furthermore, the elevated cost of rhodium imposes limitations on its widespread utilisation in platinum-rhodium alloys.

Heraeus in Germany (9) advanced the field by developing Pt-5Rh dispersion hardening (DPH) and Pt-10Rh DPH materials. These materials were formulated with zirconia, yttria and scandia serving as dispersion-strengthening phases, resulting in a notable improvement of their high-temperature performance. The Kunming Institute of Precious Metals, China, has successfully prepared Pt-5Rh oxide dispersion strengthened (ODS) and Pt-10Rh ODS materials with excellent high temperature resistance using internal oxidation combined with large plastic deformation composite rolling method (10). However, the manufacturing process of dispersion strengthened platinum materials is complex and encounters problems such as reduced welding strength, which limits their application in certain situations (11). To improve the overall performance of platinum-rhodium alloys, researchers have undertaken numerous productive endeavours. For instance, Rudnik (12) introduced platinum-based superalloys, tantalum into effectively enhancing their high-temperature strength and phase stability. However, this improvement comes at the cost of reducing the plasticity and oxidation resistance of the material. These studies indicate that solid solution strengthening and dispersion strengthening contribute to improving the mechanical properties of platinum-rhodium alloys to a certain extent.

It is worth noting that the introduction of microalloying elements into platinum-rhodium alloys may form solid solutions with the matrix,

segregate at grain boundaries or react with matrix elements to form intermetallic compounds. The interaction between alloying elements and platinum or rhodium leads to solid solution strengthening, grain refinement, precipitation strengthening and recrystallisation control effects (13). This interaction induces changes in the crystal structure and microstructure of platinum-rhodium alloys, thereby further improving their mechanical properties and high-temperature stability. Significantly, the equilibrium phase diagrams of platinum-zirconium, platinum-yttrium, rhodium-zirconium rhodium-yttrium reveal that the addition of appropriate amounts of yttrium and zirconium to platinum-rhodium alloys generates precipitation phases, including Pt<sub>5</sub>Y, Pt<sub>3</sub>Zr, RhY<sub>3</sub> and Rh<sub>3</sub>Zr (14). These phases contribute to the improvement of the mechanical properties of platinum-rhodium based alloys, while offering a simple production process and cost-effectiveness (15). Rdzawski's research demonstrated that adding 0.2% yttrium to Pt-10Rh alloy can effectively improve its mechanical properties, especially at high temperatures of 600°C (16).

Considering this, two new platinum-based alloys were designed by adding small amounts of zirconium and yttrium elements to Pt-10Rh alloy and prepared *via* arc melting and rolling processes. The microstructure and mechanical properties at room temperature and elevated temperature of these alloys were investigated. Based on the microstructure analysis, the strengthening mechanism of alloys was discussed by combining first principles and valence electron parameters calculations. The results of this study will have a positive impact on the improvement of the properties and high-temperature applications of platinum-rhodium alloys.

#### 2. Materials and Methods

#### 2.1 Experimental Methods

The Pt-10Rh-0.5Zr and Pt-10Rh-0.5Zr-0.2Y alloys were mixed according to the nominal compositions of mass percentage. The raw materials used with the purity of 99.95%, such as platinum, rhodium, zirconium and yttrium, were provided by Kunming Institute of Precious Metals. The alloy ingots were prepared by melting and casting in a vacuum arc furnace and remelted four times to ensure the uniformity of alloy composition. In order to further improve the uniformity of alloy composition, all ingots underwent a 2 h homogenisation process at 1200°C

under a vacuum of  $10^{-3}$  Pa. Subsequently, the ingots were hot-rolled to a sheet thickness of 2.0 mm at  $1100^{\circ}$ C, followed by cold rolling to 1.5 mm at room temperature. Finally, an annealing process at  $1000^{\circ}$ C for 15 min in air was applied to alleviate internal stresses from the rolled specimens.

After annealing treatment, the metallographic specimens were prepared by grinding to 4000 grit using silicon carbide paper, followed by meticulous polishing with colloidal silica suspension. Subsequently, the metallographic specimens underwent electrolytic etching using an apparatus equipped with graphite and platinum electrodes. The electrolyte solution comprised hydrochloric acid (30%) and saturated sodium chloride in a volume ratio of 3:2. The corrosion process was conducted for a duration of 1.5-3 min at a voltage of 12-15 V. The microstructure of the corroded alloys was then examined using an ECLIPSE MA200 (Nikon Corporation, Japan) OM. The Nano Measurer 1.2 grain size statistical software was applied to analyse statistically the grain size of alloy samples. The specimens underwent analysis through XRD using a D8 Advance diffractometer (Bruker, USA) equipped with a copper target. Scanning was conducted within the range of  $2\theta = 20^{\circ}$  to  $90^{\circ}$  at a scan rate of 1° min<sup>-1</sup>. The operational parameters were set with an operating current of 200 mA and an operating voltage of 40 kV. High resolution transmission electron microscopy (TEM) with model number Talos™ F200X (Thermo Fisher Scientific, USA) was adopted to analyse the microstructure of the alloys, including SAED and EDS analysis.

Tensile specimens (**Figure 1**) were fabricated by cutting pieces from rolled sheets using electrical discharge machining (EDM). The alloy samples were subjected to room temperature tensile testing using the AGS-100kNX (Shimadzu Corporation, Japan) electronic universal testing machine, with a loading rate of 3 mm min<sup>-1</sup>. High temperature tensile tests

were conducted on the TSC304B (Wance, China) high-temperature testing machine at temperatures ranging from 1300°C to 1500°C, with a heating rate of 30°C min<sup>-1</sup> and a loading rate of 0.876 mm min<sup>-1</sup>. To ensure the precision of the test outcomes, each set of specimens underwent testing three times, and the average value was considered the final result. The Vickers hardness measurements were carried out using the HXS-1000A microhardness tester with the load of 100 g. Twelve measurements were taken for each sample with uniform intervals between each test point. After removing the minimum value and the maximum value, the average hardness value of the sample was calculated, and as the final hardness value.

## 2.2 First Principle Calculation Methods

The elastic constants of the Pt<sub>5</sub>Y and zirconia phases were computed using the Cambridge Sequential Total Energy Package (CASTEP) software, based on density-functional theory, to investigate their mechanical properties. The exchange-correlation energy was treated using the generalised gradient approximation with the Perdew-Burke-Ernzerhof functional. Electron-ion interactions were described plane-wave ultrasoft pseudopotentials.  $A7 \times 7 \times 7$  Monkhorst-Pack k-point mesh was utilised to sample the first Brillouin zone, with a plane-wave cutoff energy of 500 eV. Energy convergence was achieved with an accuracy of  $1 \times 10^{-6}$  eV, and force convergence was set to -0.01 eV  $Å^{-1}$ .

#### 3. Results and Discussion

#### 3.1 Microstructure

Figure 2 presents an OM image illustrating the distinctive morphology of the Pt-10Rh based

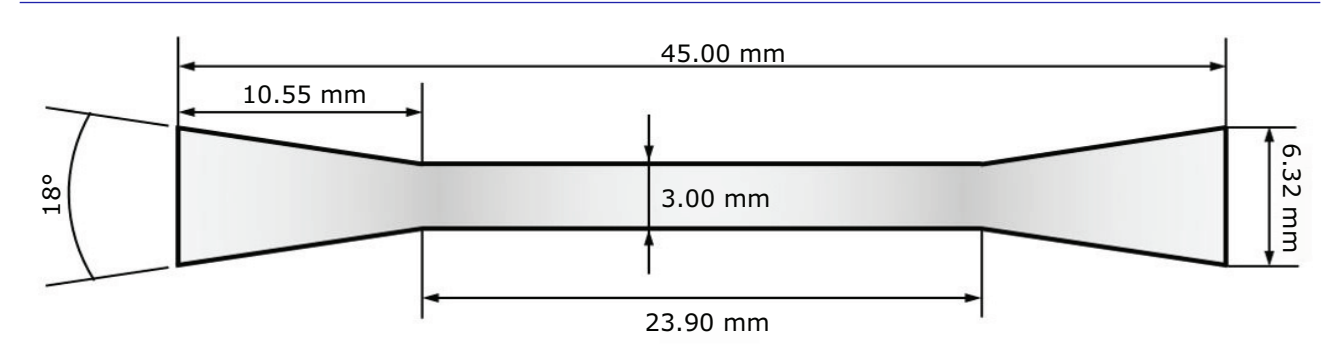


Fig. 1. Dimensions of alloy tensile samples

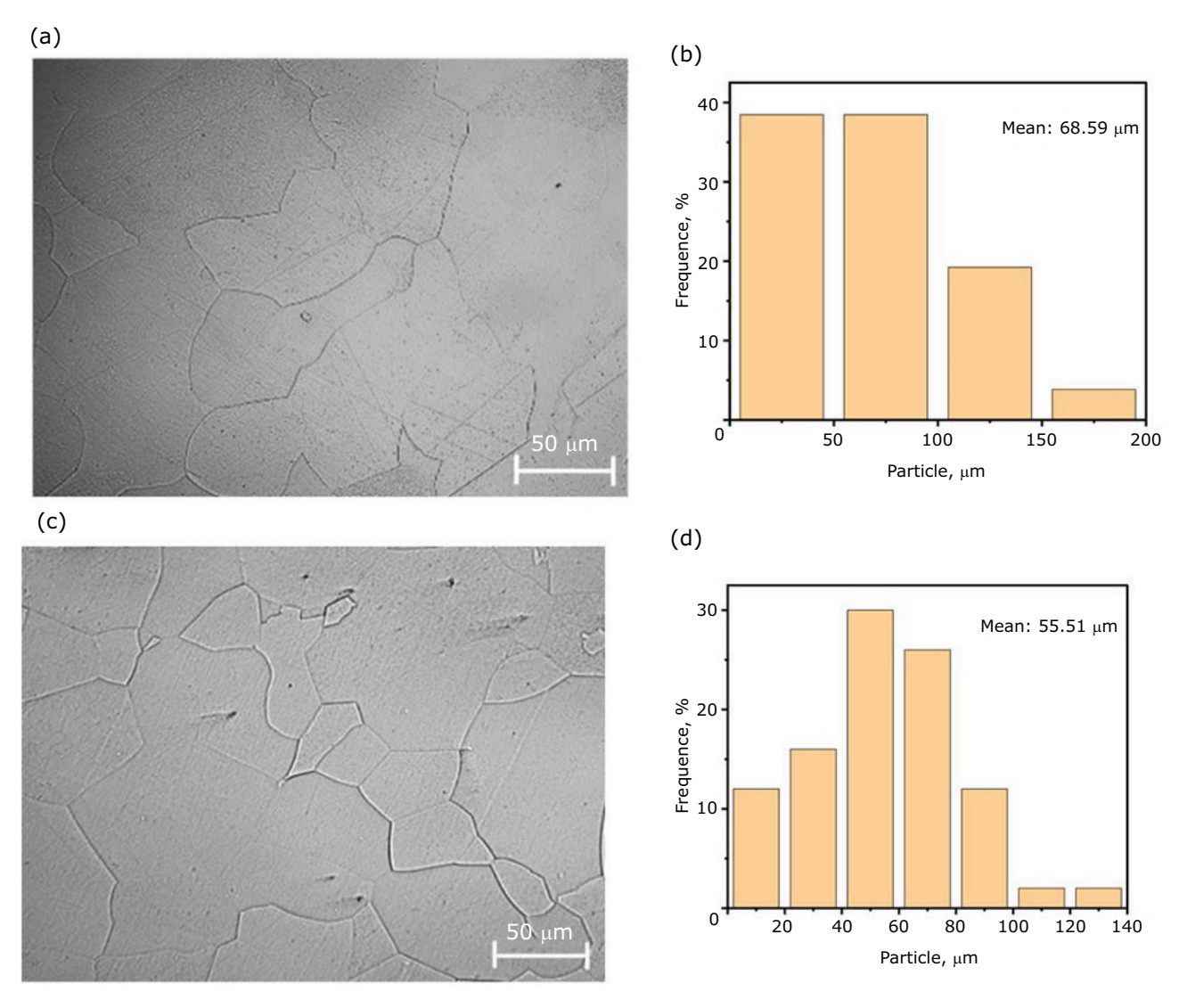


Fig. 2. (a) Metallographic structure of Pt-10Rh-0.5Zr; (b) grain distribution of Pt-10Rh-0.5Zr; (c) metallographic structure of Pt-10Rh-0.5Zr-0.2Y; (d) grain distribution of Pt-10Rh-0.5Zr-0.2Y

alloys. It is shown that the microstructures of these alloys share a fundamental resemblance, predominantly consisting of a platinum-rhodium solid solution characterised by a polygonal matrix shape. The average grain sizes of Pt-10Rh-0.5Zr and Pt-10Rh-0.5Zr-0.2Y alloys are 68.59  $\mu$ m and 55.51  $\mu$ m, respectively. This discrepancy can be attributed to the grain size-reducing effect facilitated by the addition of yttrium element (13). Moreover, no precipitates were found in the metallographic microstructure of both Pt-10Rh-0.5Zr and Pt-10Rh-0.5Zr-0.2Y alloys.

To elucidate the physical phase composition of the Pt-10Rh based alloys, an XRD test was conducted, and the results are depicted in **Figure 3**. It is shown that the matrix structure of Pt-10Rh-0.5Zr alloy is a platinum-rhodium solid solution

(platinum, rhodium), while for Pt-10Rh-0.5Zr-0.2Y alloy, besides platinum-rhodium solid solution phase, two types of oxide phases (zirconia and  $Y_{0.15}Zr_{0.85}O_{1.93}$ ) were also found to exist. However, no information on intermetallic compounds was detected in the XRD spectra of the two alloys in this work, perhaps due to the low concentration of zirconium and yttrium, resulting the number of compounds formed is very small (13).

In order to reveal the relationship between the microstructure and mechanical properties of platinum-rhodium based alloys, TEM was used to analyse the morphology, SAED and EDS of the alloys. **Figure 4** is the bright-field (BF) image and the corresponding SAED patterns of the Pt-10Rh-0.5Zr alloy. We cannot find any precipitates in the sample from the BF image in

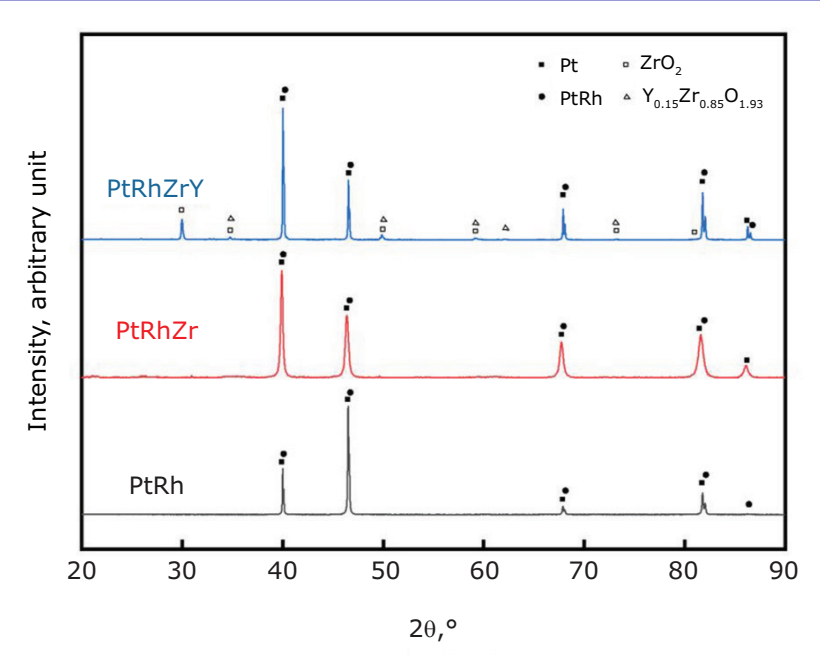


Fig. 3. The XRD patterns of Pt-10Rh-0.5Zr and Pt-10Rh-0.5Zr-0.2Y alloys

Figure 4(a). The selected diffraction super-lattice spots indexed as [110] and [100] zone axes obtained from the matrix in Figure 4(b) and 4(c) are basically invisible, indicating that there is no obvious ordered phase precipitation in the alloy. However, the zirconium peak was detected in the EDS spectrum of Figure 5, suggesting that the zirconium element may be mainly dissolved in the matrix.

The BF image and SAED patterns of Pt-10Rh-0.5Zr-0.2Y alloy are illustrated in **Figure 6**. There are still no obvious precipitates were found in the BF image of the matrix in **Figure 6(a)**. **Figure 6(b)** is the SAED pattern of region A in

the BF image, showing the diffraction spots of the platinum-rhodium solid solution. However, the precipitate phase was detected from the composite SAED pattern obtained in the region B including both matrix and precipitates, as shown in **Figure 6(c)**. Based on the SAED pattern, the precipitate phase detected is Pt<sub>5</sub>Y, which is identified as a trigonal crystal structure with the lattice parameters a = b = 5.26 Å, c = 26.32 Å and  $\gamma = 120^{\circ}$  (17).

In addition, small rod-shaped oxide particles were also found in the Pt-10Rh-0.5Zr-0.2Y alloy sample, as shown in **Figure 7**. EDS mapping shows that the distribution of zirconium and oxygen elements is relatively concentrated,

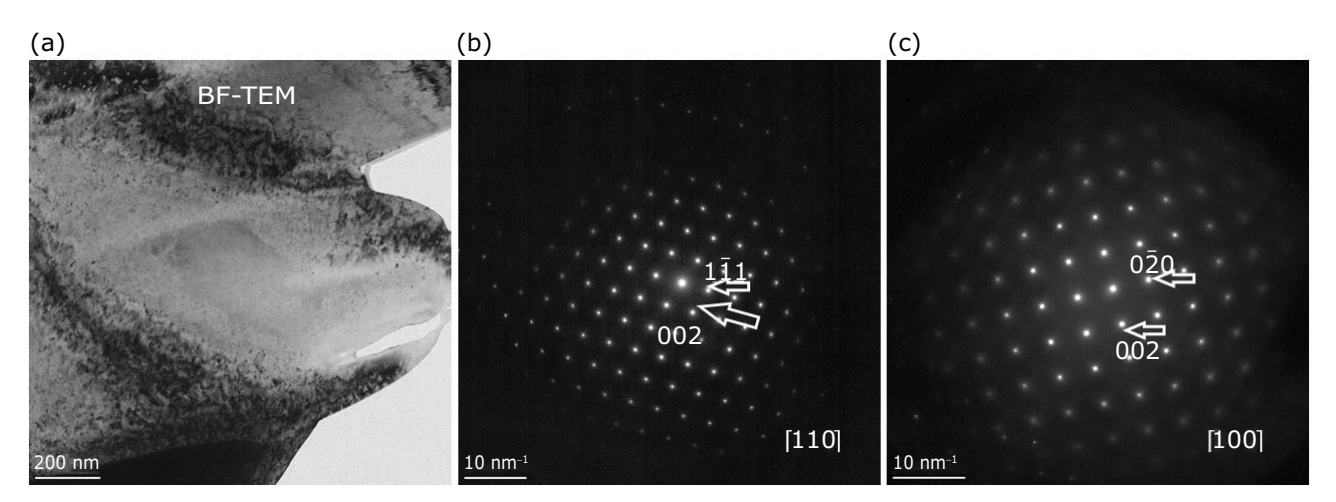


Fig. 4. BF image and SAED patterns of Pt-10Rh-0.5Zr alloy. (a) BF image of the matrix; (b) the SAED pattern along [110] zone axis; (c) the SAED pattern along [100] zone axis

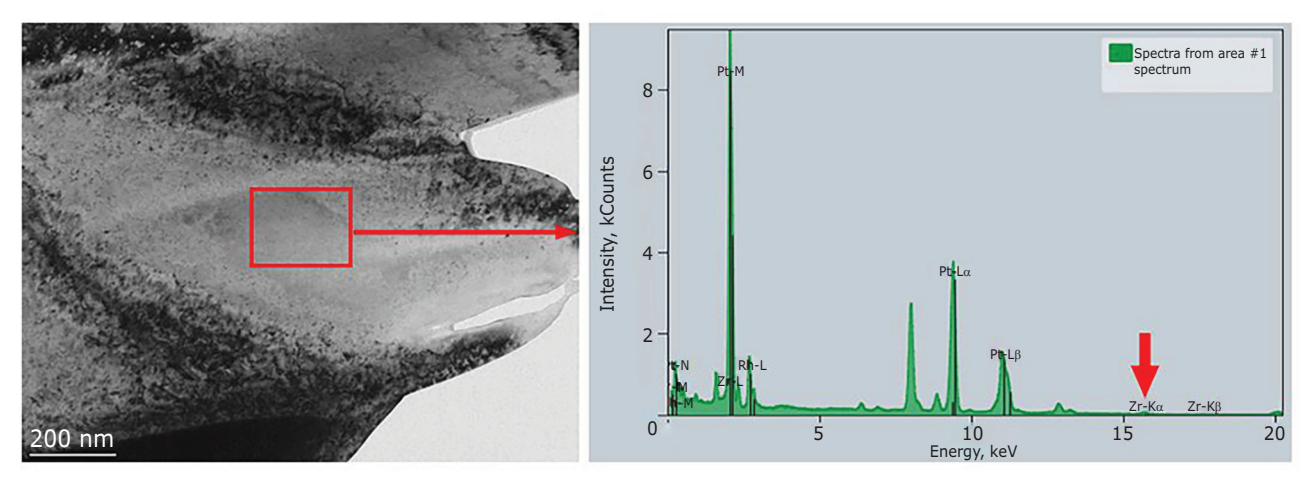


Fig. 5. EDS spectrum of Pt-10Rh-0.5Zr alloy

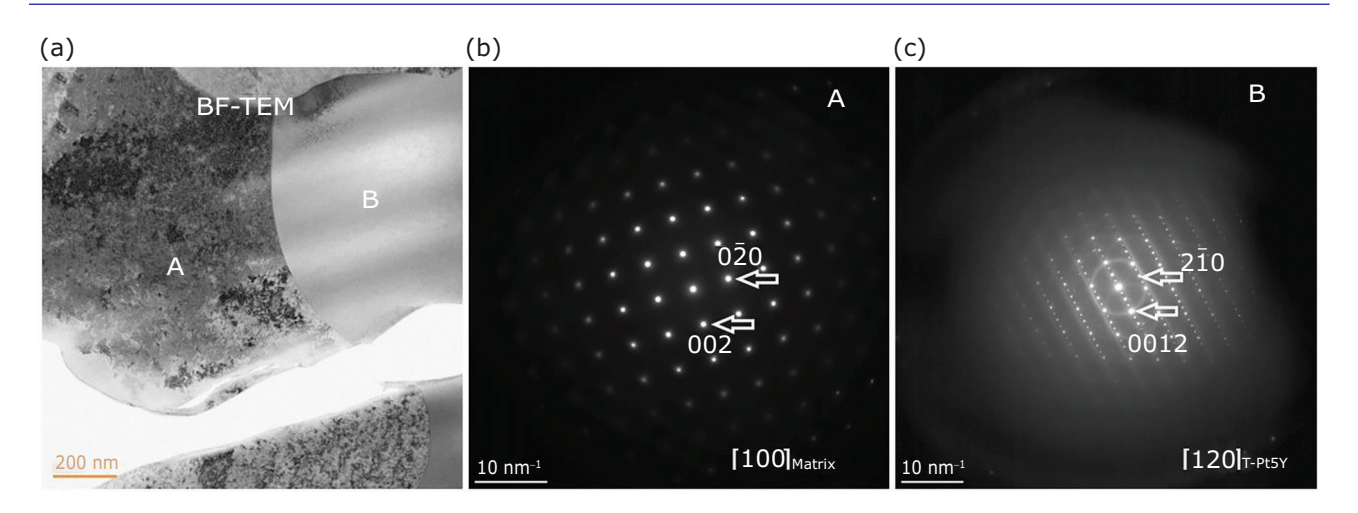


Fig. 6. (a) BF image of Pt-10Rh-0.5Zr-0.2Y alloy; (b) SAED pattern of region A; (c) SAED pattern of region B

while the content of yttrium element is very low. Therefore, it can be inferred that the formed particles are zirconium oxides, as analysed by Zhang in his research on platinum-zirconium and platinum-yttrium-zirconium alloys (13). In order to analyse the structure of oxides, SAED was performed on the oxide particle and nearby areas, as shown in Figure 8. It is speculated that the formed oxide phase (region C) is  $Zr_{0.94}Y_{0.06}O_{1.88}$ , which is basically consistent with the oxide detected by XRD, while the composition of the region near the oxide particle (region B) is a platinum-rhodium solid solution (Rh<sub>0.57</sub>Pt<sub>0.43</sub>). The above research results indicate that the addition of vttrium element is beneficial for the formation of oxides during the processing and heat treatment of the alloy in air.

#### 3.2 Mechanical Properties

The hardness values of Pt-10Rh-0.5Zr and Pt-10Rh-0.5Zr-0.2Y alloys in their original state were measured to be 154.7 HV and 163.0 HV, respectively. Compared with the hardness of 102 HV in Pt-10Rh alloy (18), adding zirconium and yttrium elements can significantly improves the Vickers hardness of Pt-10Rh alloy. Figure 9 shows the relationship between Vickers hardness and heat treatment temperature of platinum-based alloys. It can be seen that as the heat treatment temperature increases, the hardness of the alloys shows a decreasing trend. In general, as the heat treatment temperature increases, the grain size of the alloy gradually grows, and the dislocation density also decreases, leading to a decline in the hardness of the alloy.

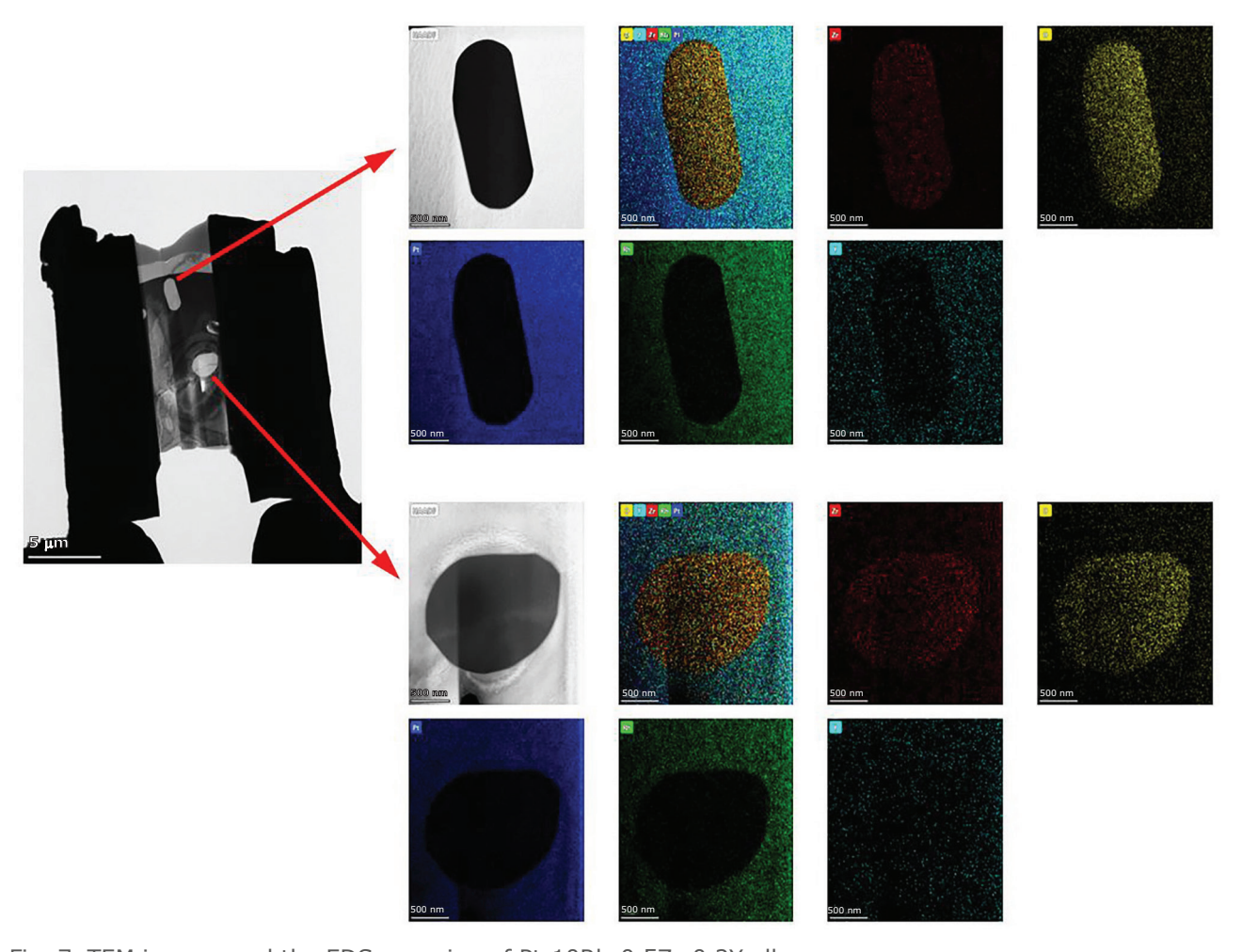


Fig. 7. TEM images and the EDS-mapping of Pt-10Rh-0.5Zr-0.2Y alloy

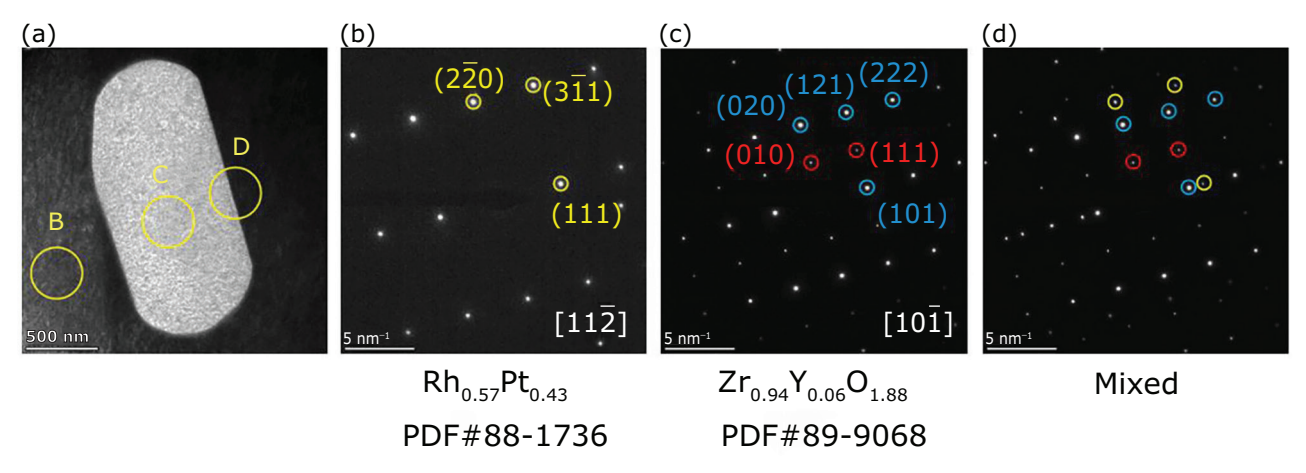


Fig. 8. (a) TEM image of the oxide particle in Pt-10Rh-0.5Zr-0.2Y alloy; (b) SAED image of region B; (c) SAED image of region C; (d) SAED image of region D

We can also see from **Figure 9** that the hardness of Pt-10Rh-0.5Zr-0.2Y remains higher than that of Pt-10Rh-0.5Zr alloy as the annealing temperature

increasing may be due to the formation of precipitate  $Pt_5Y$  and zirconium-yttrium oxides in the Pt-10Rh-0.5Zr-0.2Y alloy.

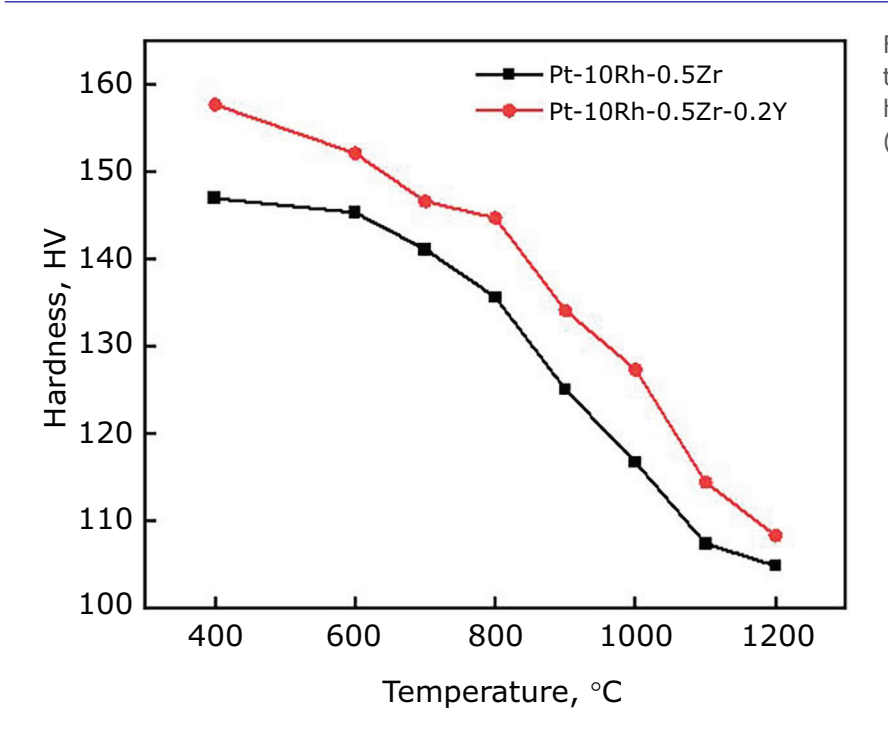


Fig. 9. The effect of heat treatment temperature on the hardness of Pt-10Rh based alloy (heat treatment time 30 min)

Table I lists the room temperature and high temperature mechanical properties platinum-based alloys. It is shown that adding a small amount of zirconium or zirconium-yttrium to Pt-10R alloy can significantly improve the mechanical properties of the alloys at room temperature and 1300°C. Compared to Pt-10Rh alloy, the ultimate tensile strength (UTS) values at room temperature of Pt-10Rh-0.5Zr-0.2Y and Pt-10Rh-0.5Zr alloys increased by 70% and 55%, while the high-temperature UTS values at 1300°C also improved by 50% and 47%, respectively. Nevertheless, we can also see from this table that as the testing temperature further increased, the UTS and elongation ( $\delta$ ) of the two platinum-based alloys showed a downward trend clearly, but the UTS values were still higher than the reported values of Pt-10Rh alloy.

It is noteworthy that there was a significant difference in UTS between the two platinum-based alloys at room temperature, but the difference at elevated temperature can be ignored. However, the high-temperature elongation of Pt-10Rh-0.5Zr-0.2Y was much higher than that of Pt-10Rh-0.5Zr. The above results indicate that yttrium has a limited high-temperature strengthening effect on platinum-rhodium based alloys, but can significantly improve the high-temperature plasticity of the alloy, which may be due to the refinement effect of yttrium on the grains.

**Figure 10** and **Figure 11** present the tensile fracture morphologies of Pt-10Rh-0.5Zr and Pt-10Rh-0.5Zr-0.2Y alloys at room temperature and 1400°C, respectively. The fracture characteristics at room temperature show a ductile fracture morphology, indicating that these two alloys have excellent room temperature plasticity. In comparison to the room temperature fracture, the micro-morphology of the Pt-10Rh-0.5Zr alloy fracture at 1400°C reveals the characteristics of cleavage fractures in specific area. Conversely, the fracture surface of Pt-10Rh-0.5Zr-0.2Y shows

Table I Mechanical Properties of Platinum-Rhodium Based Alloys									
Alloy	20°C		1300°C	1300°C		1400°C		1500°C	
	UTS, MPa	δ, %	UTS, MPa	δ, %	UTS, MPa	δ, %	UTS, MPa	δ, %	
Pt-10Rh (18)	300	38	41	15	35	30	25	35	
Pt-10Rh-0.5Zr	465	46.9	60.36	45.2	40.49	31.6	26.94	21.4	
Pt-10Rh-0.5Zr-0.2Y	510	44.7	61.46	55.1	41.52	50.8	26.86	44.3	

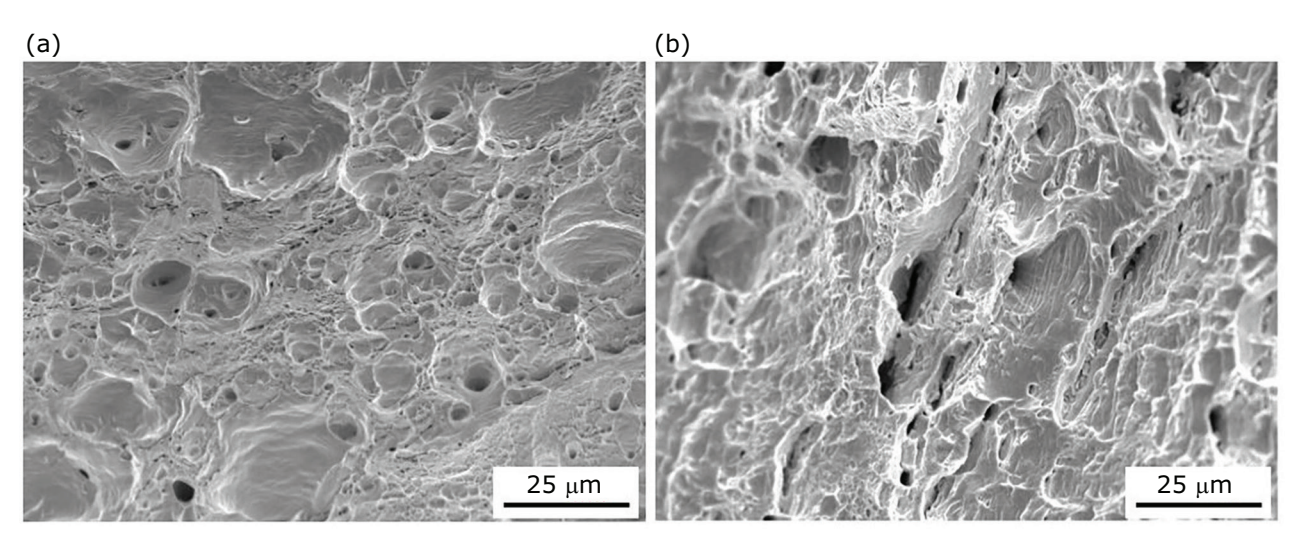


Fig. 10. Tensile fracture morphology of Pt-10Rh based alloys at room temperature: (a) Pt-10Rh-0.5Zr; (b) Pt-10Rh-0.5Zr-0.2Y

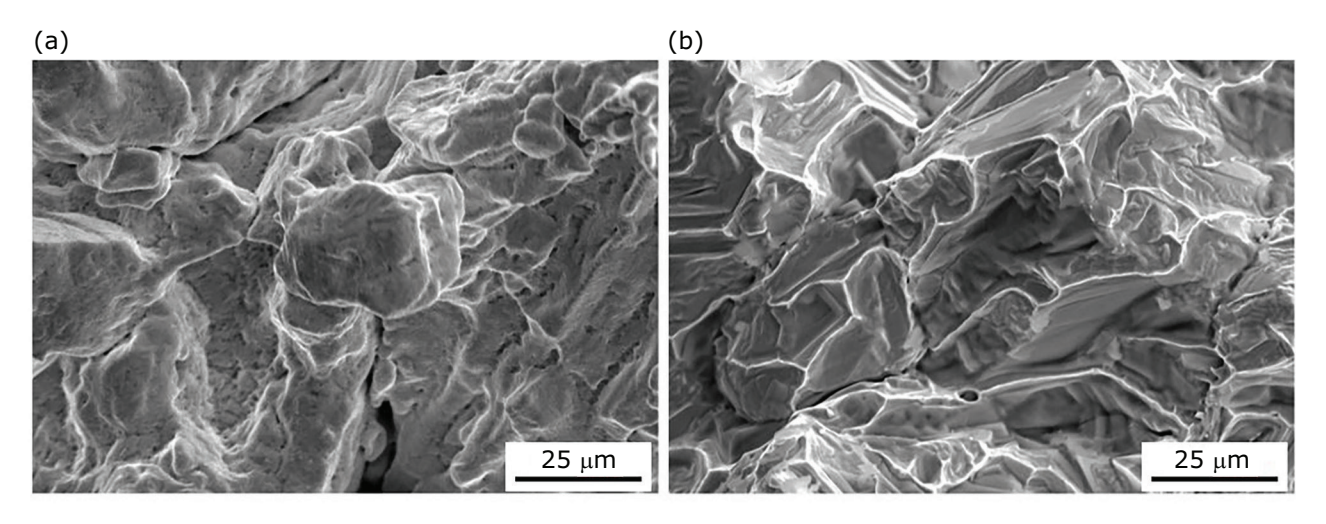


Fig. 11. Tensile fracture morphology of Pt-10Rh based alloys at  $1400^{\circ}$ C: (a) Pt-10Rh-0.5Zr; (b) Pt-10Rh-0.5Zr-0.2Y

intergranular fracture basically, which suggests that crack propagation and diffusion of the elements can occur within grains and at grain boundaries, reflecting an improvement in the alloy's plasticity.

## 3.3 Micromechanical Properties of Second Phases

The precipitated phase  $Pt_5Y$  and oxide zirconia were detected in Pt-10Rh-0.5Zr-0.2Y alloy, which may have a significant impact on the mechanical properties of the alloy. To further elucidate the intrinsic strengthening mechanism of the platinum-rhodium-zirconium-yttrium alloy by

zirconium and yttrium elements, first-principles calculations were employed in this paper to conduct an in-depth study of the mechanical properties of  $Pt_5Y$  and zirconia at the atomic scale.  $Pt_5Y$  and zirconia belong to the hexagonal and monoclinic crystal systems with space groups P6/mmm and P121/c1, respectively. Their crystal structure models and lattice constants are illustrated in **Figure 12** and detailed in **Table II**. As shown in **Table II**, the enthalpies of formation ( $\Delta H$ ) and binding energies ( $E_{coh}$ ) of  $Pt_5Y$  and zirconia are both negative, indicating that these phases can form spontaneously and possess high structural stability.

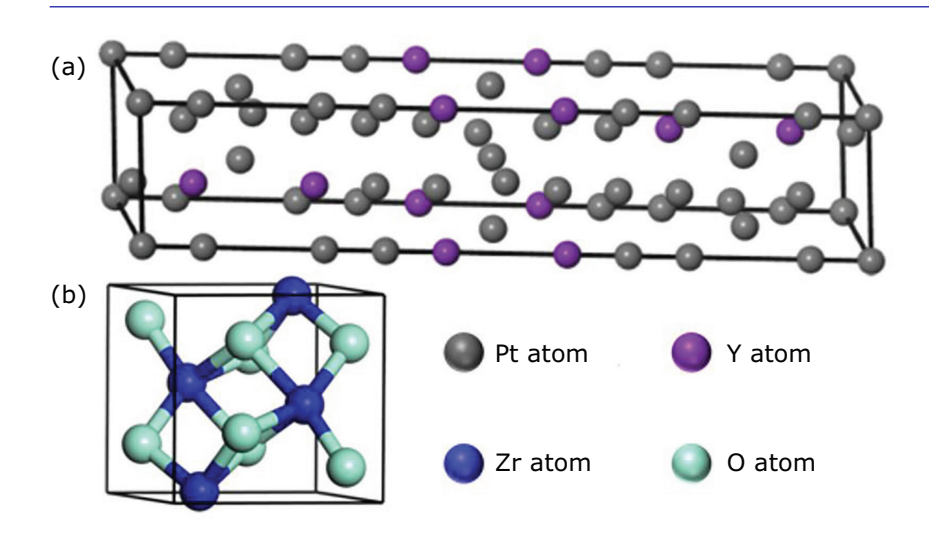


Fig. 12. Crystal structure models of: (a)  $Pt_5Y$ ; (b)  $ZrO_2$ 

Table II Lattice Constants, Binding Energy and Formation Enthalpy of Pt <sub>5</sub> Y and Zirconia									
Crystal system	Species	a, Å	b, Å	c, Å	a, °	В, °	г, °	E <sub>coh</sub> , eV atom <sup>-1</sup>	ΔH, eV atom <sup>-1</sup>
Hexagonal	Pt <sub>5</sub> Y	5.26	5.26	26.8	90.00	90.00	120.00	-6.21	-0.58
Monoclinic	ZrO <sub>2</sub>	5.15	5.22	5.32	90.00	99.43	90.00	-3.80	-10.24

To evaluate the properties and stability of  $Pt_5Y$  and zirconia, the mechanical properties, including bulk modulus (B), shear modulus (G), Young's modulus (E) and Poisson's ratio (v), were calculated (19). Using the Voigt-Reuss-Hill approximation criterion, the bulk modulus and shear modulus of these phases were determined (20–22). The results are presented in **Table III**.

**Figure 13** shows the calculated mechanical properties of  $Pt_5Y$  and zirconia. Typically, the ductility or brittleness of a crystalline material can be assessed by examining the difference in elastic constants of  $C_{12}$ – $C_{44}$ . If the value is positive, then the material is ductile; otherwise, the material is brittle. As shown in **Figure 13(a)**, both  $Pt_5Y$  and zirconia phases are ductile, with  $Pt_5Y$  exhibiting superior toughness.

Additionally, Delley characterises the brittle and ductile behaviour of materials using the ratio of bulk modulus to shear modulus  $(B_H/G_H)$  (22). When  $B_H/G_H > 1.75$ , the material is considered ductile; otherwise, it is brittle. According to the calculation results of this work, the BH/GH ratios for Pt<sub>5</sub>Y and zirconia are both greater than 1.75, indicating that they are ductile phases.

Moreover, material hardness correlates closely with its elastic-plastic behaviour, which can be predicted using a semi-empirical model:  $H_V = 2(k^2G)^{0.585}$ –3.0 (23, 24). Here k represents Boltzmann's constant, and G denotes the shear modulus. The model outcomes are illustrated in **Figure 13(b)**. It is shown that the hardness values of Pt<sub>5</sub>Y and zirconia are 6.23 GPa and 9.57 GPa, respectively, which are 73.5% and 166.6% higher than that of the Pt-10Rh matrix. It can be seen from the above analysis that both of Pt<sub>5</sub>Y and zirconia phases have high toughness and hardness and thus can be used as strengthening phases for Pt-10Rh alloys to improve the mechanical properties of the alloy.

Table III Mechanical Properties of Pt <sub>5</sub> Y and Zirconia										
Species	B, GPa			G, GPa			E, GPa	B/G	v	
Species	B <sub>V</sub>	$\mathbf{B}_{R}$	B <sub>H</sub>	$G_V$	$G_R$	G <sub>H</sub>	E	Б/Ч	V	
Pt <sub>5</sub> Y	197.72	196.37	197.04	76.16	70.16	73.16	195.32	2.69	0.33	
ZrO <sub>2</sub>	210.65	206.30	208.48	98.55	92.65	95.60	248.78	2.18	0.30	

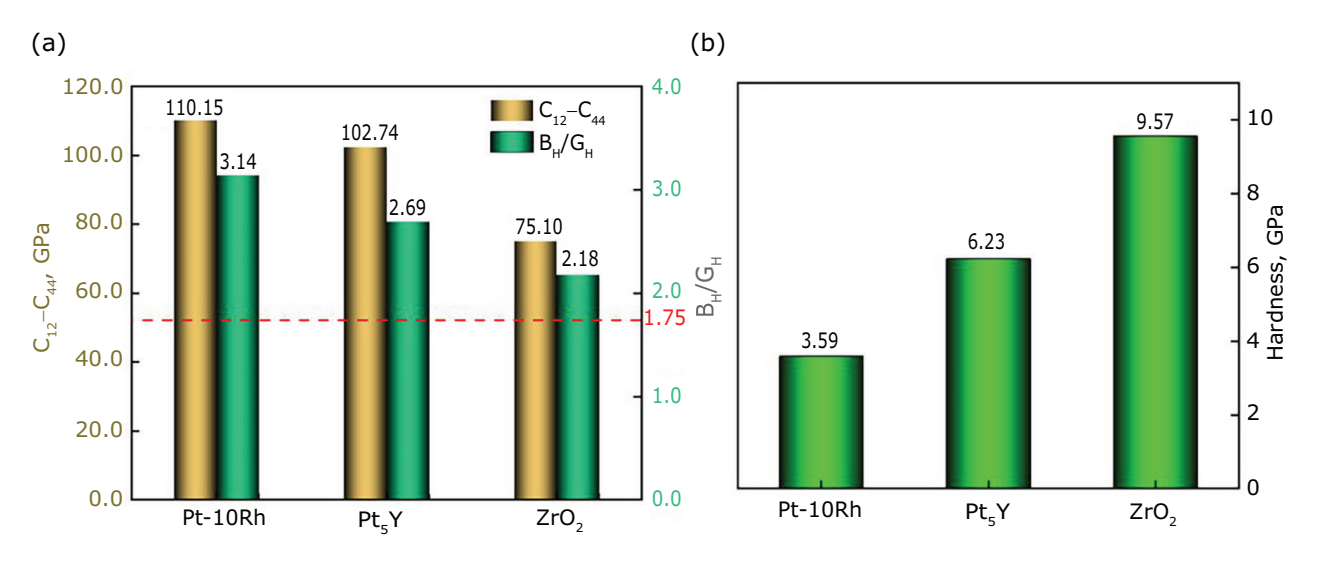


Fig. 13. Mechanical properties of Pt-10Rh, Pt<sub>5</sub>Y and ZrO<sub>2</sub>: (a)  $C_{12}$ – $C_{44}$  and  $B_H/G_H$ ; (b) theoretical hardness

## 3.4 Strengthening Mechanism of the Alloys

Compared to the Pt-10Rh alloy, Pt-10Rh-0.5Zr and Pt-10Rh-0.5Zr-0.2Y exhibit varying degrees of improvement in UTSs, particularly at room temperature and 1300°C. This enhancement is attributed to the solid solution strengthening and second phase strengthening effects. There is a larger atomic radius difference between zirconium element and platinum element, and a high solid solubility of zirconium element in the platinum matrix, which results a strong solid solution strengthening effect of zirconium on platinum-rhodium alloy (25). Moreover, the precipitate Pt<sub>5</sub>Y and dispersed zirconia particles were generated during the melting and heat treatment process in Pt-10Rh-0.5Zr-0.2Y alloy in this work. The calculation results indicate that both Pt<sub>5</sub>Y and zirconia have high toughness and hardness, which further strengthens the Pt-10Rh alloy.

Zarinejad's research shows that there is a correlation between the mechanical properties of platinum-rhodium binary alloys and their valence electron parameters (7). It was found that as the

rhodium content of the alloys increases, the valence electron number (e<sub>v</sub>) decreases and the valence electron ratio (VER) increases, resulting in an improvement in its mechanical properties such as Vickers hardness and UTS. In an attempt to further reveal the strengthening mechanism from the viewpoint of electronic structure of alloys, the valence electron parameters (e<sub>v</sub>, VER) of Pt-10Rh-0.5Zr and Pt-10Rh-05Zr-0.2Y alloys were calculated in this study and listed in Table IV. It can be seen that after adding a small amount of zirconium and zirconium-yttrium elements to Pt-10Rh alloy, the VER of the alloy remains basically unchanged, while the ev gradually decreases. This indicates that the hardness and UTS of Pt-10Rh-0.5Zr and Pt-10Rh-05Zr-0.2Y alloys increase with the decreasing of e<sub>v</sub>, seemingly independent of the alloy's VER, which is not entirely consistent with the results of the study on platinum-rhodium binary alloys in reference (7).

#### 4. Conclusions

No precipitates or oxides were found in Pt-10Rh-0.5Zr alloy, and zirconium element mainly exists uniformly in the platinum-rhodium alloy

Table IV Valence Electron Parameters and Mechanical Properties of Platinum-Rhodium Based Alloys								
Pt-Rh, wt%	Pt-Rh, at%	$e_v$	VER	Hardness, HV	UTS, MPa			
Pt-10Rh (7)	Pt-17.4Rh	9.826	0.136	79	292.3			
Pt-10Rh-0.5Zr	Pt-17.3Rh-1.0Zr	9.768	0.1358	154.7	465			
Pt-10Rh-0.5Zr-0.2Y	Pt-17.2Rh-1.0Zr-0.4Y	9.741	0.1357	163.0	510			

matrix in solid solution form. However, second phases were detected in the Pt-10Rh-0.5Zr-0.2Y alloy, including the precipitate phase  $Pt_5Y$  with a triangular crystal structure and the zirconium yttrium oxide phases of  $ZrO_2$ ,  $Zr_{0.94}Y_{0.06}O_{1.88}$ .

Pt-10Rh-0.5Zr-0.2Y UTSs of and Pt-10Rh-0.5Zr alloys experienced varying degrees of enhancement compared to Pt-10Rh, with improvements of 70% and 55% at room temperature, and 50% and 47% at 1300°C, respectively. As the testing temperature further increased to 1500°C, the UTS of the two platinum-rhodium based alloys remained higher than that of Pt-10Rh alloy. Pt-10Rh-0.5Zr-0.2Y has higher UTS and high-temperature plasticity.

The zirconium element dissolved in the platinum matrix has a strong solid solution strengthening effect on Pt-10Rh alloy, while the  $Pt_5Y$  precipitate phase and zirconium or zirconium-yttrium oxides formed during the preparation process with high toughness and hardness further strengthen the alloy. The mechanical properties of platinum-rhodium based alloys are related to their valence electron number, that is, as the valence electron number decreases, the hardness and UTS of the alloys increase.

#### **Acknowledgments**

This work is supported by Science and Technology Projects in Yunnan Province (202203ZA080001, 202302AB080021), Key Project of Yunnan Precious Metals Laboratory Co Ltd (No.YPML-2023050213, YPML-2022050215) and the National Natural Science Foundation of China (52161005).

#### References

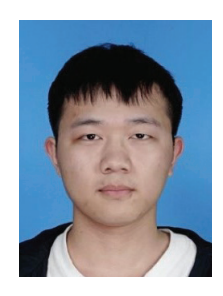
- 1. J. H. Potgieter, N. B. Maledi, M. Sephton, L. A. Cornish, *Platinum Metals Rev.*, 2010, **54**, (2), 112
- L. A. Cornish, R. Süss, L. H. Chown, A. Douglas, M. Matema, L. Glaner, G. Willams, 'New Pt-Based Alloys for High Temperature Application in Aggressive Environments: The Next Stage', Second International Platinum Conference: Platinum Surges Ahead, Sun City, South Africa, 8th-12th October, 2006, Symposium Series S45, The Southern African Institute of Mining and Metallurgy, Johannesburg, South Africa, 2006, pp. 57-66

- 3. L. A. Cornish, R. Süss, L. H. Chown, L. Glaner, *Platinum Metals Rev.*, 2009, **53**, (3), 155
- 4. L. A. Cornish, R. Süss, A. Douglas, L. H. Chown, L. Glaner, *Platinum Metals Rev.*, 2009, **53**, (1), 2
- B. Fischer, D. Freund, A. Behrends, D. F. Lupton, J. Merker, *Erzmetall*, 1998, **51**, (6), 429
- P. J. Hill, L. A. Cornish, G. B. Fairbank, *JOM*, 2001,
  53, (10), 19
- 7. M. Zarinejad, S. Rimaz, Y. Tong, K. Wada, F. Pahlevani, *Johnson Matthey Technol. Rev.*, 2023, **67**, (3), 290
- 8. S. Zhonghua, P. Xiaodong, X. Weidong, L. Weiting, Y. Zonglun, *Rare Met. Mater. Eng.*, 2012, **41**, (3), 402
- 9. G. L. Selman, J. G. Day, A. A. Bourne, *Platinum Metals Rev.*, 1974, **18**, (2), 46
- J. M. Zhang, Y. H. Geng, S. Chen, W. M. Guan, K. H. Zhang, *Mater. Rep.*, 2009, 23, (3), 58
- 11. R. G. Stanley, F. G. Wilson, *Met. Powder Rep.*, 1982, **37**, (4), 175
- 12. Y. Rudnik, R. Völkl, S. Vorberg, U. Glatzel, *Mater. Sci. Eng. A*, 2008, **479**, (1–2), 306
- 13. Q. Zhang, D. Zhang, S. Jia, W. Shong, *Platinum Metals Rev.*, 1995, **39**, (4), 167
- "Binary Alloy Phase Diagrams", 2nd Edn., eds. T.
  B. Massalski, H. Okamoto, P. R. Subramanian, L. Kacprzak, 3 volumes, ASM International, Ohio, USA, 1990, 3589 pp
- 15. P. J. Meschter, W. L. Worrell, *Metall. Trans. A*, 1977, **8**, (3), 503
- 16. Z. M. Rdzawski, J. P. Stobrawa, *J. Mater. Process. Technol.*, 2004, **153–154**, 681
- 17. H. Ge, X. Gan, L. Fu, B. Zhang, J. He, Y. Wei, Y. Mao, *Scr. Mater.*, 2024, **243**, 115990
- 18. 'PtRh10', Heraeus Precious Metals, Hanau, Germany, September, 2021
- 19. M. Sanati, R. C. Albers, T. Lookman, A. Saxena, *Phys. Rev. B*, 2011, **84**, (1), 014116
- 20. A. Reuss, Z. Angew. Math. Mech., 1929, 9, (1), 49
- 21. R. Hill, Proc. Phys. Soc. A, 1952, 65, (5), 349
- 22. H. Liu, S. Zhang, J. Zhang, Q. Ren, L. Zhang, Y. Ge, *Mater. Today Commun.*, 2023, **34**, 105118
- 23. B. D. Fulcher, X. Y. Cui, B. Delley, C. Stampfl, *Phys. Rev. B*, 2012, **85**, (18), 184106
- 24. X.-Q. Chen, H. Niu, D. Li, Y. Li, *Intermetallics*, 2011, **19**, (9), 1275
- 25. Y. Ning, Z. Yang, F. Wen, "Platinum", Metallurgical Industry Press, Beijing, China, 2010

#### The Authors



Professor Changyi Hu studied Material Physics and Chemistry at Central South University in China and obtained a doctoral degree. He has been engaged in high-temperature material research at Kunming Institute of Precious Metals, China, for a long time. His main research interests are precious metal high-temperature alloys, coatings and refractory metal materials applied in the aerospace field.



Xiangxing Xiao is a current Master's student at the Kunming Institute of Precious Metals. He is currently working on precious metal high-temperature alloys and refractory multiprincipal alloys.



Qianqi Wei is a Researcher in the Research and Development Center of Kunming Institute of Precious Metals. He is skilled in the preparation, structure and performance research of high-temperature alloys. Currently, he is working in the field of precious metal processing and applications.



Junmei Guo is a Professor at the Kunming Institute of Precious Metals. She got her Master's degree in Materials Science from Kunming Institute of Precious Metals. Her research interests are advanced precious metal alloys, catalytic materials and recycling of secondary resources. She has published more than 10 papers in SCI journals recently.



Xian Wang is a Researcher in the Research and Development Center of Kunming Institute of Precious Metals. He carries out modelling and simulation in computation materials science, and is currently working on finite element simulation and analysis, as well as database building of precious metal materials.



Li Chen is the Deputy Director of Kunming Institute of Precious Metals. He is a Principal Engineer of genome project of precious metal alloy materials in the Alloy Material Group, where he is working on first-principles calculations, database building of precious metal alloys and new high-temperature materials.



Professor Hongzhong Cai is a Senior Researcher in the High Temperature Materials Division at Kunming Institute of Precious Metals. He is working on films or coatings of platinum group metals and ceramics, as well as structural materials of refractory metals prepared by chemical vapour deposition.



Xuehang Wang is an Assistant Engineer of Kunming Institute of Precious Metals. His research focuses on the development of rare and precious metal materials and high-temperature alloys, with particular emphasis on mechanical property evaluation and materials processing technologies for advanced structural applications.



Xiaohong Yuan is an Associate Professor, as the director of physical properties testing department of Kunming Institute of Precious Metals. Her main research areas include the analysis, testing and structural characterisation of platinum group metal alloys, refractory metals, steel and aluminium alloys.



Yan Wei acquired a doctoral degree in engineering from Kunming University of Science and Technology in China. Now, she is a Professor at Kunming Institute of Precious Metals, as well as the Head of High Temperature Materials Division at State Key Laboratory of Platinum Metal Functional Materials, China. Her main fields of research include alloys of platinum group metals, refractory metals and coatings.



Zhentao Yuan is an Associate Professor at Kunming University of Science and Technology. He has been engaged in research on the design, surface modification and application of rare and precious metal materials. He participated in and led multiple projects funded by the National Natural Science Foundation of China.